FEBS 29675 FEBS Letters 579 (2005) 3651–3659

Comparison of replicative senescence and stress-induced premature senescence combining differential display and low-density DNA arrays

Thierry Pascal[a], Florence Debacq-Chainiaux[a], Aline Chrétien[a], Coralie Bastin[a], Anne-France Dabée[a], Vincent Bertholet[b], José Remacle[a,b], Olivier Toussaint[a,*]

[a] *Unit of Research on Cellular Biology (URBC), Department of Biology, University of Namur (FUNDP), Rue de Bruxelles, 61 B-5000 Namur, Belgium*
[b] *Eppendorf Array Technologies (EAT), Belgium*

Received 17 February 2005; revised 14 April 2005; accepted 23 May 2005

Available online 8 June 2005

Edited by Michael Sussman

Abstract Human diploid fibroblasts (HDFs) exposed to subcytotoxic stress display many features of senescence. Using differential display RT-PCR, gene expression of HDFs in premature senescence induced by *tert*-butylhydroperoxide or ethanol and in replicative senescence was compared to gene expression of HDFs at early cumulative population doublings. Thirty genes of known function were identified from the 265 differentially displayed cDNA fragments. A customized low-density array allowed to confirm the relative level of the corresponding 30 transcripts. We found differential expression of genes coding for proteins implicated namely in growth arrest (*PTEN*, *IGFBP-3*, *LRP-1* and *CAV1*), senescent morphogenesis (TGF-β1 and *LOXL2*) and iron metabolism (*TFR* and *FTL*).

Keywords: Ageing; Stress; Ethanol; Reactive oxygen species; Gene expression; TGF-β1

1. Introduction

Limited mitotic life span is observed in many eukaryotic cell types and is interpreted as a manifestation of cellular ageing. Irreversible growth arrest at the G1/S phase of the cell cycle is namely due to the overexpression of cyclin-dependent kinase inhibitors such as $p21^{waf-1}$ and $p16^{ink4a}$, leading to hypophosphorylation of the retinoblastoma protein. Human diploid fibroblasts (HDFs) in replicative senescence (RS) are characterized by a typically enlarged cell shape, senescence-associated β-galactosidase (S-A β-gal) activity, short telomeres and changes in the expression level of many genes (for a review: [1]). HDFs exposed to subcytotoxic concentrations of agents such as *tert*-butylhydroperoxide (*t*-BHP) [2–5], hydrogen peroxide (H_2O_2) [6] and ethanol [2,3,5], or with subcytotoxic doses of UV- [7] and UVB- [8], become postmitotic and display many biomarkers of senescence within two to three days after stress. This has been termed stress-induced premature senescence (SIPS) (for a review: [9]). Many RS-related alteration of the steady-state level of specific transcripts are known [10–14]. A limited set of genes was discovered to undergo similar changes of mRNA abundance in SIPS induced by oxidative agents and in RS (for a review: [15]).

In the present study, we wished to know whether premature senescence induced by exposures of WI-38 foetal lung HDFs to subcytotoxic doses of *t*-BHP [2–5] or ethanol [2,3,5] involves long-term changes in gene expression similar to those found in RS. Differential display RT-PCR (DD RT-PCR) is a simple open transcriptomic approach for identifying transcripts with different abundance in several experimental conditions [16,17]. Given this method potentially generates false positives, the results were confirmed with a customized low-density DNA array. The reliability of this technology has been fully demonstrated previously [8,18,19]. Also this technology was already used successfully in different models of SIPS: H_2O_2-induced premature senescence of skin HDFs ectopically expressing telomerase or not [19] and UV-B-induced premature senescence of skin HDFs [8]. Nevertheless, we confirmed a relevant proportion of the results with real-time RT-PCR.

2. Materials and methods

2.1. Cell culture and induction of SIPS

WI-38 foetal lung HDFs (AG06814, Coriell Cell Repositories, USA) were routinely subcultivated in basal medium Eagle (BME) (Invitrogen) supplemented with 10% foetal calf serum (FCS) (Invitrogen) as previously described [20]. The medium was changed every 4 days in slowly growing cultures. Cells unable to make a population doubling within two weeks were considered as replicatively senescent. Subconfluent HDFs at 60% of their proliferative life span were exposed 5 times for 1 h to 30 μM *t*-BHP (Merck) or 5 times for 2 h to 5% ethanol (v/v) (Merck) freshly diluted in BME + 10% FCS, with a stress per day for five days. At the end of each stress, the HDFs were rinsed with PBS buffer and provided with fresh BME + 10% FCS. Control cells were submitted to identical experimental conditions, in the absence of stressing agent [2–4].

2.2. Differential display

At 72 h after the last stress, total RNA was extracted (Total RNA-gent extraction kit, Promega). 10 μg of total RNA were treated with 5 U of RNase-free DNase I (Invitrogen). Starting with 0.2 μg of

*Corresponding author. Fax: +32 81 724135.
E-mail address: olivier.toussaint@fundp.ac.be (O. Toussaint).

Abbreviations: HDFs, human diploid fibroblasts; RS, replicative senescence; SIPS, stress-induced premature senescence; *t*-BHP, *tert*-butylhydroperoxide; EtOH, Ethanol; PTEN, phosphatase and tensin homolog; IGFBP-3, insulin-like growth factor binding protein-3; LRP-1, lipoprotein-related protein 1; TFR, transferrin; FTL, ferritin light chain polypetide; TGF-β1, transforming growth factor-β1; LOXL2, lysyl oxidase-like 2; MAPK, mitogen-activated protein kinase

0014-5793/$30.00
doi:10.1016/j.febslet.2005.05.056

DNA-free total RNA, cDNAs were synthetized using 200 U Superscript II Reverse Transcriptase (Invitrogen) in the presence of 1 μM of a two-base anchored primer $T_{16}VA$, $T_{16}VC$, $T_{16}VG$ or $T_{16}VT$ (where V = A, C or G). The cDNA was amplified in a subsequent PCR with the *Taq* gold polymerase (Perkin–Elmer) in the presence of 1 μCi of [α-^{33}P]dATP (NEN Life Science). The PCR conditions were: 10 min at 94 °C followed by 4 cycles at low annealing temperature (94 °C for 30 s, 40 °C for 1 min, 72 °C for 2 min) followed by 40 cycles (94 °C for 30 s, 60 °C for 1 min, 72 °C for 2 min). A set of 15 arbitrary primers, from 18 to 24 bases long (Table 1, Panel B) was used in combination with 4 two-base anchored poly-T primers (Table 1, Panel A) generating 60 PCR mix for each set of samples. Amplified products were separated on a 8% polyacrylamide gel electrophoresis in the presence of 7 M urea. The gels were recorded by film autoradiography. The cDNAs differentially displayed in at least one of the four experimental situations were excised from the dried gels, rehydrated, reamplified and cloned in pGEM-T easy vector (Promega). The purified plasmids were sequenced (ABI PRISM Dye Terminator sequencing, Perkin–Elmer) using the M13 forward (GTAAAACGACGGCCAGT) and M13 reverse (GGAAACAGCTATGACCATG) primers. Sequence homology was determined using the BLAST algorithm against the nucleotide databases (nr) at the National Center for Biotechnology Information (NCBI) at http://www.ncbi.nlm.nih.gov/BLAST.

2.3. Real time RT-PCR

At 72 h after the last stress, total RNA was extracted from independent cultures. After RNA extraction, cDNA was synthetized using 200 U Superscript II Reverse Transcriptase (Invitrogen) in the presence of 1 μg of oligo dT_{12-18} (Invitrogen). Amplification reaction assays contained 1× SYBR Green PCR Mastermix and primers (Applied Biosystems, Table 1, Panel C) at optimal concentrations. A hot start at 95 °C for 5 min was followed by 40 cycles at 95 °C for 15 s and 65 ° for 1 min using the 7000 SDS thermal cycler (Applied Biosystems). Melting curves were generated after amplification. Each sample was tested in triplicate.

2.4. Low-density DNA arrays, synthesis of labeled DNA and hybridization conditions

Before grafting on glass slides, the sequences of the DNA capture probes were carefully chosen by sequence comparison. We controlled experimentally that no cross-hybridization took place. Two arrays (a control and a test) were spotted per glass slide with three identical subarrays per array. Positive and negative hybridization and detection controls were spotted on each subarrays in order to control the reliability of the experimental data, as previously reported [8,18,19].

Table 1
Sequences of the primers used in DD RT-PCR analysis (Panels A and B) and real-time RT-PCR analysis (Panel C)

Name	Sequence
Panel A: Two bases anchored polyT primers	
$T_{16}VA$	CGGCTGCAGTTTTTTTTTTTTTTTTVA
$T_{16}VT$	CGGCTGCAGTTTTTTTTTTTTTTTTVT
$T_{16}VC$	CGGCIGCAGTTTTTTTTTTTTTTTTVC
$T_{16}VG$	CGGCIGCAGTTTTTTTTTTTTTTTTVG

Name	Sequence
Panel B: Arbitrary primers	
AP01	CGACAATGCTGGACTGACACACG
AP02	ATTGAGACTGAGGTGAACATTAGC
AP03	GAGATAGACACATAGATACGAGC
AP04	CTCACTACGGCTCGCTACTCG
AP05	GCTGTGCGAAGTGACCATCCTCC
AP06	GTAGTCTAAGCGTTGGAGTTCA
AP07	CTACCTTTGCCGAGCCAGTTA
AP08	CTTCGGTTGTTACGGATGC
AP09	GGGGCTAATCTGCTTCGGT
AP10	ATCTGAGGTACTGTCCGC
AP11	GCCTCATCCTGTAGACTAGCTG
AP12	CTGCTAGATGGATGTGTACG
AP13	GCATGGCGGCTCCTGGACTA
AP14	AAGTCAGGGTCTATCAAGCG
AP15	TGATGCTACTGTAACCTGATGCG

Abbreviations	GenBank	Forward primer	Reverse primer
Panel C			
APOJ	NM_001831	GGATGAAGGACCAGTGTGACAAG	CAGCGACCTGGAGGGATTC
APOL	NM_030882	TGAGGCCTGGAACGGATTC	TTGCAAGGTTGTCCAGAGCTTTA
AUP1	NM_012103	CGCAAGAAGGAGATTCACAGAGA	GGGTGCCATCCTGTTCCTTT
BIRC6	NM_016252	GCAGCTCTCAAGCGTCACACT	TTAGAGTCTCCTCAGCACCTGTTG
CAV1	NM_001753	CGCACACCAAGGAGATCGA	GTGTCCCTTCTGGTTCTGCAAT
ES1	NM_004649	GAGGCTTTGGAGCGGCTAA	GCCTGGTGGAACTCCTTCAG
FTL	NM_000146	CCGTCAACAGCCTGGTCAA	GCCTTCCAGAGCCACATCA
IGFBP3	NM_000598	CAGAGCACAGATACCCAGAACTTC	CACATTGAGGAACTTCAGGTGATT
KPNB1	NM_002265	TGTACAGCATTTGGGAAGGATGT	TCGATCTCCGCCCTTCAGT
LOXL2	NM_002318	CTCCAACAACATCATGAAATGCA	TGCTCAAACTTTTTTTCCGTCTCT
OSTEO	NM_003118	GAGACCTGTGACCTGGACAATG	GGAAGGAGTGGATTTAGATCACAAGA
PTEN	NM_000314	TGGATTCAAAGCATAAAAACCATTAC	GTCTTCAAAAGGATATTGTGCAACTCT
RPL13A	NM_012423	CTCAAGGTCGTGCGTCTGAA	TGGCTGTCACTGCCTGGTACT
S100A13	XM_371380	CTCAGCGTCAACGAGTTCAAAG	CCAAGCTCTTCATCTTCTCATCAA
S100A4	NM_002961	CGCTTCTTCTTTCTTGGTTTGATC	CCCTCTTTGCCCGAGTACTTG
TFR	NM_003234	ACAATGCTGCTTTCCCTTTCC	TCAGTTCCTTATAGGTGTCCATGGT
TGF-β1	NM_000660	AGGGCTACCATGCCAACTTCT	CCGGGTTATGCTGGTTGTACA

10 μg of total RNA were retrotranscribed using SuperScript II Reverse Transcriptase (Invitrogen). Six synthetic poly(A) + tailed RNA standards were spiked at three different amounts (0.1, 1 and 10 ng per reaction) into the purified RNA.

Triplicates from three independent experiments were performed, meaning hybridizations on nine subarrays. Hybridization was carried out following Eppendorf's instructions as reported [8,18,19]. Detection was performed using a Cy3-conjugated IgG anti-biotin (Jackson Immuno Research Laboratories).

2.5. Imaging, data normalization and statistical analysis

The fluorescence of the hybridized arrays was scanned (Packard ScanArray, Perkin–Elmer) at a 10 μM resolution. To maximize the dynamic range of detection, the same arrays were scanned at three photomultiplier gains (50, 70, 100) for quantifying high, medium and low amounts of hybridized cDNAs. The scanned 16-bit images were imported into the ImaGene 4.1 software (BioDiscovery). The fluorescence intensity of each DNA spot (average of intensity of each pixel present within spot) was calculated using local mean background subtraction. A signal was accepted when the average intensity after background subtraction was at least 2.5-fold higher than its local background. The three intensity values of the triplicate DNA spots were averaged and used to calculate the intensity ratio between the reference and the test samples. The data were normalized in two steps. First, the values were corrected considering the intensity ratios of the internal standards spiked into the references and test samples. The presence of the 6 internal standards probes at two different locations on the array allowed to consider the local background and array homogeneity in the normalization. However, to ensure that the amount of cDNA hybridized was the same for each array, a second step of normalization was performed based on calculating the average intensity for a set of 8 housekeeping genes. This set of multiple housekeeping genes, with different expression levels, was preferred to a single reference gene to avoid any bias due to possible variability of the expression level of a single housekeeping gene. The 8 genes considered for normalization of the data code for 23 kDa highly basic protein, beta-actin, aldolase A, cyclophylin E, glyceraldehyde-3-phosphate dehydrogenase, hexokinase I, hypoxanthine phosphoribosyltransferase and ribosomal protein S9. These reference genes are widely used in the scientific community for signal normalization [8,18,19,21–24]. The global ratios obtained for the 8 housekeeping genes when comparing RS or SIPS to HDFs at early CPDs in three independent experiments were: 0.96 ± 0.13 for RS, 1.20 ± 0.20 for *t*-BHP-induced premature senescence and 1.17 ± 0.21 for ethanol-induced premature senescence. The variance of the normalized set of housekeeping genes was used to generate an estimate of expected variance, leading to a predicted confidence interval for testing the significance of the ratios obtained. Ratios outside the 95% confidence interval were determined to be significantly different [8,18,19].

3. Results

3.1. DD RT-PCR analysis

Total RNA was extracted from WI-38 HDFs in RS or in premature senescence induced by a series of five exposures to *t*-BHP or ethanol, at a respective concentration of 30 μM and 5% v/v as described in Section 2. These subcytotoxic stresses induced the appearance of several biomarkers of senescence as shown previously [2–4]. We confirmed that these conditions increased sharply the percentage of S.A. β-Gal positive cells and dramatically decreased the level of [^{3}H]-thymidine incorporation into DNA (not shown). We used DD RT-PCR in order to identify gene transcripts with changed abundance in HDFs in RS and/or in SIPS. Sixty primers combinations made of 4 two bases anchored poly-T primers (Table 1, Panel A) and 15 arbitrary primers (Table 1, Panel B) were used for RT-PCR. Differential display patterns (Fig. 1A) were obtained displaying each an average of 200 bands in each condition. Analysis of the patterns (Fig. 1B) revealed 147 cDNA fragments with differential abundance between young and replicatively senescent HDFs, including 77 RS-specific variations and 70 variations common between RS and SIPS induced by *t*-BHP and/or ethanol. Respectively 66 and 72 other bands were differentially displayed in SIPS induced either by *t*-BHP and/or ethanol, when compared to control HDFs, with 20 commonly differentially displayed bands after exposure to both types of stress. The differentially displayed cDNA fragments were recovered from the gels and re-amplified by using the corresponding pair of primers, before cloning and sequencing. A total of 141 cDNA fragments were sequenced. Homology searches (BLAST, NCBI) led to the identification of 95 cDNA fragments including 18 redundant identifications. Thus 77 transcript species were identified (Table 2). These results were sorted into genes of known (Table 2A) and unknown (Table 2B) function. We focused on the genes of known function, bearing in mind that this subset of genes could give clues on the establishment of the senescent phenotype.

3.2. Low-density DNA array

Given DD RT-PCR analysis can generate false positives [16], we confirmed these results by two complementary methods: customized low-density DNA arrays and real-time RT-PCR.

A customized low-density DNA array consisting of 35 cDNA capture probes of interest, as well as 6 internal standards, a set of 8 housekeeping genes, hybridization and detection controls, covalently linked on a glass slide, was designed as previously described [8,18,19,25]. Among the 35 genes of interest were the 30 candidates of known function identified after DD RT-PCR analysis (Table 2A) and 5 genes commonly overexpressed in RS or SIPS: apolipoprotein J (apo J), fibronectin, osteonectin, transforming growth factor-beta 1 (TGF-β1) and caveolin-1. Apo J has an extracellular chaperone-like activity similar to small heat shock proteins [26,27]. Fibronectin is an essential component of the extracellular matrix and may contribute to the morphological changes observed in senescent HDFs as well as anchorage of cells to their substrate [28]. Osteonectin is a calcium-binding protein able to inhibit the cell entry into S phase through selective binding of platelet-derived growth factor (PDGF) [29]. TGF-β1 is a pleiotropic cytokine involved in many cell functions like growth and differentiation. More specifically, TGF-β1 controls the appearance of several biomarkers of cellular senescence after exposure of HDFs to subcytotoxic stress with H_2O_2 or UVB [6,8]. Caveolin-1, the structural protein component of caveolar membranes, is a scaffolding protein that concentrates, organizes, and functionally modulates signalling molecules. Caveolin-1 was shown to be overexpressed in premature senescence of NIH-3T3 murine fibroblasts [30]. An increase of the level of caveolin-1 triggers a senescent-like phenotype in murine and human diploid fibroblasts [30–32].

The customized DNA array-based analysis allowed to measure the abundance of these 35 transcripts in all the experimental situations (Fig. 1C) and eliminate the false positives generated by DD RT-PCR (Table 3).

Although the reliability of the technology of low-density DNA array used herein was fully demonstrated, most of the results obtained with the customized DNA array were confirmed by real-time RT-PCR. No discrepancy of the sense of variation was observed between the arrays and the real-time RT-PCR results, as previously reported for this type of arrays [8,18,19].

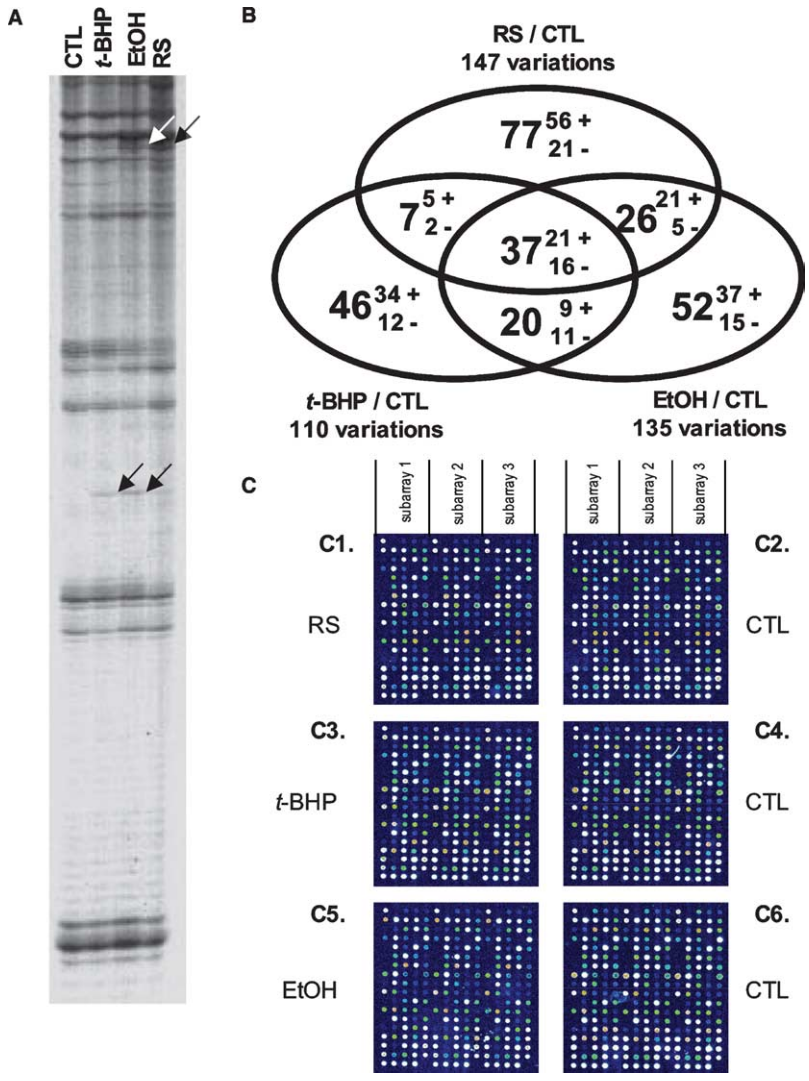

Fig. 1. (A) A portion of typical differential display patterns is shown. cDNA fragments were obtained from total RNA for HDFs controls (CTL), in *t*-BHP induced premature senescence, in ethanol induced premature senescence and in replicative senescence. The arrows indicate cDNA bands with higher intensities. (B) Sorting of the numbers of cDNA fragments displaying variations of intensities on the autoradiographies according to the experimental condition (increase (+) or decrease (−) of intensity). (C) Representative example of images obtained with the low-density DNA arrays scanned at gain 100 of the photomultiplier. Each array features spots in triplicate (subarrays). Three arrays were used in each condition. C1: replicative senescence; C3: *t*-BHP induced premature senescence; C5: ethanol induced premature senescence; C2, C4 and C6: respective controls.

The results obtained with the customized DNA array also confirmed that apo J, fibronectin, osteonectin, TGF-β1 and caveolin-1 were all found overexpressed in RS and in both kinds of SIPS, confirming previous results found with different methods in RS and in *t*-BHP-induced premature senescence [4,6,8,30,31]. This further validated our strategy combining DD RT-PCR with these customized low-density DNA arrays. Based on these robust results and on the previous knowledge accumulated on RS and SIPS, we analysed the possible role of these novel changes in gene expression found in RS and/or SIPS.

4. Discussion

This comparison of gene expression reinforces the notion that, despite displaying a wide variety of common biomarkers of senescence at the morphological, biochemical and gene expression levels, RS and SIPS are not alike. This was already shown previously at the transcriptional level in H_2O_2- [19] and at the protein level in *t*-BHP- and ethanol-induced premature senescence [2,3]. We also discovered a novel set of ethanol regulated genes.

The overexpression of apo J, osteonectin and fibronectin observed in *t*-BHP-induced premature senescence confirms previous results [4]. Apo J has already been shown to increase the resistance of cells against SIPS. Indeed ectopically-induced overexpression of apo J decreases sharply the appearance of the biomarkers of senescence after exposures of HDFs to *t*-BHP, ethanol [5] and UVB [8]. Osteonectin overexpression inhibits PDGF-induced proliferation of HDFs [5] whereas fibronectin overexpression was suggested to favour the senescent morphogenesis and the anchorage of the cells to their substrate, explaining their resistance to apoptosis [4]. Very

Table 2
Transcripts identified after DD RT-PCR analysis of RS and SIPS

Band#	GenBank	Identification	ΔRS	Δ*t*-BHP	ΔEtOH
Panel A: Transcripts which corresponding cDNA was grafted on the customized low-density DNA arrays for further verification of their expression level					
03C4	NM_005731	Actin related protein 2/3 complex, subunit 2	Down	Down	Down
03A1	NM_012103	*Ancient ubiquitous protein 1*	Up	Up	Up
03G2	NM_012103	*Ancient ubiquitous protein 1*	Up	Up	Up
05G2	NM_002318	Lysyl oxidase-like 2	Up	Up	Up
05G3	NM_002568	Poly(A) binding protein, cytoplasmic 1	Up	Up	Up
13T2	NM_002961	S100 calcium binding protein A4	Up	Up	Up
14C1	NM_003234	Transferrin receptor	Up	Up	Up
06G1	NM_006623	Phosphoglycerate dehydrogenase	Down	Down	Down
07G4	NM_002873	RAD17 homoiog (*S. pombe*)	Down	Down	Down
08C3	NM_001402	Eukaryotic translation elongation factor 1 alpha 1	Up	Up	Up
08T4	NM_017913	Hsp90-associating relative of Cdc37	Down	Down	Down
09T1	NM_000027	Aspartylglucosaminidase	Up	Up	Up
10A3	NM_000146	*Ferritin, light polypeptide*	Up	Up	Up
10G1	NM_000146	*Ferritin, light polypeptide*	Up	Up	Up
10G2	NM_000146	*Ferritin, light polypeptide*	Up	Up	Up
10T1	NM_000146	*Ferritin, light polypeptide*	Up	Up	Up
15G3	NM_016252	Baculoviral IAP repeat-containing 6	Up	Up	Up
03T1	XM_290506	Splicing factor 3b, subunit 2	Up	Up	
03T2	NM_021103	Thymosin, beta 10	Up		Up
04G3	NM_000314	Phosphatase and tensin homolog	Up		Up
06A1	XM_371380	*S100 calcium binding protein A13*	Down		Down
06A2	XM_371380	*S100 calcium binding protein A13*	Down		Down
08C1	NM_015577	Retinoic acid induced 14	Up		Up
08C1	NM_002265	*Karyopherin beta 1*	Up		Up
08C4	NM_002265	*Karyopherin ES1*	Up		Up
15A1	NM_004649	*Mitochondrial precursor ES1*	Up		Up
15A2	NM_004649	*Mitochondrial precursor ES1*	Up		Up
10A4	NM_021259	Transmembrane protein 8 (five membrane-spanning domains)	Up	Up	
04A5	NM_012091	Adenosine deaminase, tRNA-specific 1	Down		
04T2	NM_015571	SUMO-1-specific protease	Up		
04T3	NM_006801	KDEL (Lys-Asp-Glu-Leu) endoplasmic reticulum protein retention receptor 1	Up		
06C1	NM_000598	Insulin-like growth factor binding protein 3	Up		
12G4	NM_002332	Low-density lipoprotein-related protein 1	Up		
15C2	NM_015484	*GCIP-interacting protein p29*	Up		
15C3	NM_015484	*GCIP-interacting protein p29*	Up		
15G2	NM_015484	*GCIP-interacting protein p29*	Up		
15G1	NM_030882	Apolipoprotein L, 2	Up		
08T2	NM_002951	Ribophorin II		Down	
11G1	NM_004749	Cell cycle progression 2 protein			Up
Panel B: Other transcripts					
01C1	XM_007615	Ribosomal protein S17	Down	Down	Down
01G2	AC048334	BAC RP11-572C15 from chromosome 3	Up	Up	Up
03A2	AC008670	Clone CTB-36O1 from chromosome 5	Down	Down	Down
03C1	NM_000998	*Ribosomal protein L37a*	Up	Up	Up
03G1	NM_000998	*Ribosomal protein L37a*	Up	Up	Up
11T1	NM_000998	*Ribosomal protein L37a*	Up	Up	Up
09A1	NM_001015	*Ribosomal protein 311*	Up	Up	Up
09G1	NM_001015	*Ribosomal protein S11*	Up	Up	Up
09A3	AL022719	Clone RP1-231L4 from chromosome Xq27. 1-27.3	Up	Up	Up
09T3	NM_012090	Microtubule-actin crosslinking factor 1	Up	Up	Up
10T2	XM_290799	*KIAA 1501 protein*	Down	Down	Down
10T5	XM_290799	*KIAA 1501 protein*	Down	Down	Down
10T6	XM_290799	*KIAA 1501 protein*	Down	Down	Down
04G2	AC005552	Clone hRPK.212_E_8 from chromosome 17	Up		Up
06C4	XM_007889	Hypothetical protein FLJ10640	Down		Down
11A2	XM_012945	Hypothetical protein FLJ11168	Up		Up
11C1	XM_058968	Hypothetical protein FLJ20897	Up		Up
12A1	XM_005146	Hypothetical protein FLJ20327	Up		Up
12A2	AC020896	Clone CTC-347C20 from chromosome 5	Up		Up
03T8	AL121852	BAC R-159L20 of library RPCI-11 from chromosome 14		Down	Down
05C8	AC005156	PAC clone RP5-1099C19 from 7q21-q22		Down	Down
08T1	AC093117	Clone RP11-86H7 from chromosome 1		Down	Down
12G3	NM_005243	Ewing sarcoma breakpoint region 1		Down	Down
12T1	NM_021645	KIAA0266 gene product		Up	Up
15A4	BC013294	DKFZP564O0823 protein		Up	Up
04A2	AC006255	PAC RPCI5-1087L12 from chromosome 3p21.1-9	Up		
04C3	NM_004233	CD83 antigen	Down		
04G5	AL355836	BAC R-8L8 of library RPCI-11 from chromosome 14	Up		

(*continued on next page*)

Table 2 (*continued*)

Band#	GenBank	Identification	ΔRS	Δ*t*-BHP	ΔEtOH
04G6	AC007227	Clone RPCI-11_54H19 from chromosome 1	Up		
04T1	AL031848	Clone RP1-202O8 from chromosome 1p36.11-36.31	Up		
05T2	AC002122	Clone GS1-293J4 from 5p15.2	Down		
06A3	AY011168	*16S ribosomal RNA gene*	Up		
06T1	AY011168	*16S ribosomal RNA gene*	Up		
06T2	AY011168	*16S ribosomal RNA gene*	Up		
06C2	AF130342	Clone PAC 87.1 from chromosome 8q24.1	Up		
07C2	NM_016211	Yeast Sec31p homolog	Up		
07G1	AC005664	PAC Clone p965k14 from Chromosome 22q11	Up		
07G3	AL122089	cDNA DKFZp566J2324	Up		
08C2	NM_017967	*Hypothetical protein FLJ20850*	Down		
08C5	NM_017967	*Hypothetical protein FLJ20850*	Down		
08G1	AF277191	PNAS-133	Up		
08G2	AL035409	Clone RP4-564M11 from chromosome 1p31.1	Up		
09A2	NM_024863	Hypothetical protein FLJ21174	Up		
10C1	AC004934	PAC clone RP5-953B5 from chromosome 7	Up		
10C2	AL445190	Clone RP11-349J5 from chromosome 6	Up		
10G5	AL121929	Clone RP11-416N2 from chromosome 10	Up		
10T3	NM_001388	Developmentally regulated GTP-binding protein 2	Up		
11A1	AL110197	cDNA DKFZp586J021	Up		
11G4	NM_016030	Tetratricopeptide repeat domain 15	Up		
12G2	NM_015949	Chromosome 7 open reading frame 20			Up
11G5	AL137059	Clone RP11-125123 from chromosome 13	Up		
12G5	BC061520	CGI-130	Up		
15C1	Z95331	Clone CTA-941F9 from chromosome 22q13	Down		
10G4	NM_015414	*Ribosomal protein L36*			Down
10T4	NM_015414	*Ribosomal protein L36*			Down
11G3	AC003098	Clone HRPC905N1 from chromosome 17			Up

Band number, GenBank number, name and sense of variation (Δ) observed according to the experimental condition studied are given. In italic: cDNA fragments with redundant identifications.

interestingly, we discovered that these genes are also overexpressed in premature senescence induced by ethanol.

H_2O_2 at subcytotoxic concentration induces irreversible growth arrest and triggers the overexpression of caveolin-1 in NIH-3T3 cells. This is greatly reduced when the cells harbor antisense caveolin-1. The induction of growth arrest is reactivated after restoration of the level of caveolin-1 [30]. For the first time, we describe an overexpression of caveolin-1 in premature senescence of normal HDFs and its ethanol-modulated regulation.

TGF-β1 is overexpressed respectively by skin and foetal lung HDFs after a series of exposures to UVB [8] and after a single exposure to H_2O_2 [6]. TGF-β1 overexpression is necessary for the overexpression of apo J, osteonectin, fibronectin and TGF-β1 itself, namely via a positive feed-back on the activation of $p38^{MAPK}$ [33]. We now report that TGF-β1 is also overexpressed in *t*-BHP- and ethanol-induced premature senescence and in RS of WI-38 HDFs. This broadens the role of TGF-β1 in SIPS and RS. In addition, we report that two TGF-β1-related genes are overexpressed in *t*-BHP- and ethanol-induced premature senescence and/or in RS: insulin-like growth factor-binding protein-3 (IGFBP-3) and low-density lipoprotein-related protein 1 (LRP1). TGF-β1 stimulates the synthesis and secretion of IGFBP-3 by HDFs [34]. IGFBP-3 expression is associated with inhibition of cell proliferation and cellular senescence (for a review: [35]). LRP-1 is another name of the type V TGF-β receptor. Interestingly, LRP-1 is required for the growth arrest induced by IGFBP-3 and TGF-β1 [36–38]. Lastly IGFBP-3 is also overexpressed in UVB-induced premature senescence of skin HDFs [8].

We also report a relative increase of the steady-state level of ferritin light chain polypeptide (FTL), transferrin receptor (TFR), lysyl oxidase-like 2 (LOXL2), PTEN tumour suppressor and S100A4. Ferritin, transferrin and TFR participate in the decrease of the concentration of free iron. Free iron is a catalyst of the reactive oxygen species generated in the Fenton reaction [39]. Noteworthy, TFR participates in the cellular internalization of IGFBP-3 via the binding of IGFBP-3 to transferrin [40]. LOXL2, a member of lysyl oxidase family, is a secreted enzyme that initiates the cross-linking of collagens and elastin, thereby altering the extracellular matrix [41]. The steady-state mRNA level of the tumour suppressor PTEN increased in RS. This phosphatase converts phosphatidylinositol 3,4,5-triphosphate (PIP_3) into PIP_2. A decrease of PIP_3 upregulates $p27^{kip1}$, a cyclin-dependent kinase inhibitor responsible for growth arrest [42,43].

Lastly, we found that S100A4 is overexpressed in RS. This is a Ca^{++} binding protein specifically expressed in fibroblasts. Its overexpression causes an increase of cell surface [44], as observed in RS.

The customized low-density DNA arrays allowed to eliminate the false positives generated by DD RT-PCR. It also allowed to determine whether the changes suspected with DD RT-PCR in a given phenotype also exist in the other phenotypes under study. This approach can be generalized to any biological model where a given cell type can exist in different states.

Further studies could be aimed at determining whether the changes observed herein at the transcript level can also be found at the protein level. Nevertheless this study, together with the proteome analysis performed on the same models of RS and SIPS, and in the same experimental conditions [3], shows that the regulation of the expression of genes involved in various metabolic pathways, cell functions or cell components is altered in RS and/or SIPS. The proteomic study previously performed on WI-38 HDFs in SIPS induced by *t*-BHP or ethanol focused

Table 3
List of transcripts found with changed abundance in RS and in *t*-BHP or ethanol-induced SIPS

Abbreviations	GenBank	Name	Function	ΔDD RT-PCR	ΔArray	ΔReal-time RT-PCR
Replicative senescence						
APOJ	NM_001831	**ApolipoproteinJ**	**Stress Response**		**1.8 ± 0.2**	**2.7 ± 0.4**
APOL	NM_003661	Apolipoprotein L	Lipid metabolism	UP	UP	14.6 ± 1.3
AUP1	NM_012103	Ancient ubiquitous protein 1	Signal Transduction		1.9 ± 0.3	2.4 ± 0.4
BIRC6	NM_016252	Baculoviral IAP repeat-containing 6 (apollon)	Apoptosis (−)	UP	1.9 ± 0.2	1.6 ± 0.1
CAV1	NM_001753	**caveolin 1, caveolae protein, 22 kDa**	**Transport**		**2.2 ± 0.4**	**2.6 ± 0.6**
EEF1A1L14	NM_001403	Eukaryotic translation elongation factor 1 alpha 1-like 14	Translation	UP	1.8 ± 0.1	
ES1	NM_004649	Mitochondrial precursor ES1	Mitochondrial protein precursor	UP	1.5 ± 0.1	1.7 ± 0.2
FN1	NM_002026	**Fibronectin**	**Extracellular matrix**		**1.7 ± 0.1**	
FTL	NM_000146	Ferritin, light polypeptide	Cell homeostasis		1.6 ± 0.1	2.4 ± 0.2
IGFBP3	NM_000598	Insulin-like growth factor binding proteins	Cytokines and growth factors	UP	2.6 ± 0.2	4.1 ± 0.3
KDELR1	NM_006801	KDEL endoplasmic reticulum protein retention receptor 1	Intracellular protein traffic	UP	1.7 ± 0.2	
KPNB1	NM_002265	Karyopherin (importin) beta 1	Intracellular protein traffic	UP	1.8 ± 0.2	1.7 ± 0.1
LOXL2	NM_002318	Lysyl oxidase-like 2	Extracellular matrix	UP	2.3 ± 0.4	3.2 ± 0.7
LRP1	NM_002332	Low-density lipoprotein-related protein 1	Receptor	UP	1.7 ± 0.3	
OSTEO	NM_003118	**Osteonectin**	**Extracellular matrix**		**1.7 ± 0.1**	**2.1 ± 0.3**
PABPC1	NM_002568	Poly(A)-binding protein, cytoplasmic 1	RNA processing	UP	1.9 ± 0.3	
14-3-3-ZETA	NM_003406	14-3-3-ZETA	Signal Transduction	UP	2.1 ± 0.3	
PTEN	NM_000314	Phosphatase and tensin nomolog (tumor suppressor)	Cell cycle	UP	2.1 ± 0.3	5.1 ± 0.7
S100A4	NM_002961	S100 calcium binding protein A4	Calcium binding		2.0 ± 0.3	
TFR	NM_003234	Transferrin receptor	Transport		1.9 ± 0.1	5.7 ± 0.9
TGFβ1	NM_000660	**TGF-beta1**	**Cytokines and growth factors**		**1.5 ± 0.1**	**2.0 ± 0.3**
TMSB10	NM_021103	Thymosin beta 10	Cytoskeleton	UP	1.6 ± 0.3	
ARPC2	NM_005731	Actin related protein 2/3 complex, subunit 2 34kD	Cytoskeleton	DOWN	−2.1 ± 0.3	
HARC	NM_017913	Hsp90-associating relative of Cdc37	Chaperone	DOWN	−2.8 ± 0.3	
PHGDH	NM_006623	Phosphoglycerate dehydrogenase	Serine biosynthesis	DOWN	−3.3 ± 0.3	
ADAT1	NM_012091	*Adenosine deaminase, t-RNA specific 1*	*RNA processing*	*DOWN*	*1.9 ± 0.1*	
S100A13	NM_005979	*S100 calcium-binding protein A13*	*Calcium binding*	*DOWN*	*2.0 ± 0.4*	*6.0 ± 0.7*
t-BHP induced SIPS						
APOJ	NM_001831	**ApolipoproteinJ**	**Stress Response**		**1.6 ± 0.1**	**1.6 ± 0.1**
CAV1	NM_001753	**Caveolin 1, caveolae protein, 22 kDa**	**Transport**		**1.5 ± 0.0**	**1.5 ± 0.1**
FN1	NM_002026	**Fibronectin**	**Extracellular matrix**		**1.7 ± 0.0**	
FTL	NM_000146	Ferritin, light polypeptide	Cell homeostasis	UP	1.6 ± 0.2	1.5 ± 0.1
IGFBP3	NM_000598	Insulin-like growth factor binding protein3	Cytokines and growth factors		2.4 ± 0.3	1.9 ± 0.2
LOXL2	NM_002318	Lysyl oxidase-like 2	Extracellular matrix	UP	1.6 ± 0.2	2.5 ± 0.4
OSTEO	NM_003118	**Osteonectin**	**Extracellular matrix**		**1.8 ± 0.3**	**1.5 ± 0.1**
TFR	NM_003234	Transferrin receptor	Receptor		2.1 ± 0.3	3.1 ± 0.7
TGFβ1	NM_000660	**TGF-beta1**	**Cytokines and growth factors**		**1.7 ± 0.2**	**1.5 ± 0.1**
ADAT1	NM_012091	Adenosine deaminase, *t*-RNA specific 1	RNA processing		−1.8 ± 0.2	
HARC	NM_017913	HSP90-associating relative of Cdc37	Chaperone	DOWN	−1.7 ± 0.1	
EtOH induced SIPS						
APOJ	NM_001831	**ApolipoproteinJ**	**Stress Response**		**1.9 ± 0.1**	**2.0 ± 0.3**
CAV1	NM_001753	**Caveolin 1, caveolae protein, 22 kDa**	**Transport**		**1.8 ± 0.1**	**2.4 ± 0.2**
FN1	NM_002026	**Fibronectin**	**Extracellular matrix**		**1.9 ± 0.2**	
FTL	NM_000146	Ferritin, light polypeptide	Cell homeostasis	UP	1.6 ± 0.0	1.6 ± 0.1
IGFBP3	NM_000598	Insulin-like growth factor binding proteins	Cytokines and growth factors		2.2 ± 0.2	2.6 ± 0.4
LOXL2	NM_002318	Lysyl oxidase-like 2	Extracellular matrix	UP	1.7 ± 0.3	2.6 ± 0.6
OSTEO	NM_003118	**Osteonectin**	**Extracellular matrix**		**2.0 ± 0.2**	**1.5 ± 0.2**
S100A4	NM_002961	S100 calcium binding protein A4	Calcium binding		1.7 ± 0.2	
TFR	NM_003234	Transferrin receptor	Receptor		1.8 ± 0.2	5.2 ± 0.9
TGFβ1	NM_000660	**TGF-beta1**	**Cytokines and growth factors**		**1.6 ± 0.1**	**1.6 ± 0.1**
ADAT1	NM_012091	Adenosine deaminase, *t*-RNA specific 1	RNA processing		−2.5 ± 0.2	
HARC	NM_017913	HSP90-associating relative of Cdc37	Chaperone	DOWN	−1.8 ± 0.2	

Correspondence between the sense of variation found with DD RT-PCR and array. Italic letters: DD RT-PCR false positives. Bold letters: biomarkers of senescence and SIPS. ΔDD RT-PCR: increase (UP) or decrease (DOWN) of cDNAs on autoradiographies of gels separating DD RT-PCR amplicons identified in this experimental condition. ΔArray: fold-increase or -decrease (−) of the abundance of transcripts as found with low-density DNA arrays after statistical analysis of the results obtained from 3 independent experiments. UP: transcript not detected in HDFs at early CPDs. ΔReal-time RT-PCR: fold-change of abundancy of transcripts found for the results verified with real-time RT-PCR.

on highly expressed hydrophilic proteins undergoing neosynthesis and/or post-translational modifications [3]. Despite these limitations, that study found a 35% decrease of the abundance of glucose-6-phosphate-1-dehydrogenase (G6PD) in RS and a 50% increase of the abundance of pyruvate kinase M in RS and ethanol-induced premature senescence [3]. The latter is a key regulatory enzyme of glycolysis. An overexpression of the alpha-enolase, another enzyme involved in glycolysis was also observed in RS [3]. These data partly explain why the glycolytic activity is increased in RS [45]. An overexpression of the heat shock protein 27 and of the antioxidant protein peroxiredoxin VI was also found [3]. An overexpression of the $p21^{waf-1}$ cyclin-dependent kinase inhibitor was described previously in *t*-BHP-induced premature senescence [4], explaining the hypophosphorylation of the retinoblastoma protein and growth arrest [46]. Our study suggests that genes coding for proteins indirectly involved in growth arrest are also involved (osteonectin, PTEN, IGFBP-3, LRP-1, caveolin-1), as well as genes coding for proteins playing a role in iron metabolism (TFR, ferritin), morphogenesis and extracellular matrix (fibronectin, TGF-β1, LOXL2).

These results confirm that the senescent phenotype, whether induced replicatively or prematurely by stress, is complex since several cellular functions are affected at the same time, probably through numerous cross-talking signaling pathways.

Acknowledgments: F. Debacq-Chainiaux and O. Toussaint are respectively Research Assistant and Research Associate of the FNRS, Belgium. We acknowledge the Region Wallonne/FSE project "Arrayage" (EPH 3310300 R0472/215316). We also thank Dr. J. Campisi and Dr. K. Itahana (Lawrence Berkeley National Laboratory, Berkeley, CA, USA) for providing the initial protocols for differential display RT-PCR, and Dr. F. de Longueville (Eppendorf Array Technologies, Namur, Belgium) for providing protocols for constructing the low-density DNA arrays used in this study.

References

[1] Campisi, J. (1999) Replicative senescence and immortalization in: The Molecular Basis of Cell Cycle and Growth Control (Stein, A., Baserga, A., Giordano, A. and Denherdt, D.T., Eds.), pp. 348–373, Wiley, New York.

[2] Dierick, J.F., Eliaers, F., Remacle, J., Raes, M., Fey, S.J., Larsen, P.M. and Toussaint, O. (2002) Stress-induced premature senescence and replicative senescence are different phenotypes, proteomic evidence. Biochem. Pharmacol. 64, 1011–1017.

[3] Dierick, J.F., Kalume, D.E., Wenders, F., Salmon, M., Dieu, M., Raes, M., Roepstorff, P. and Toussaint, O. (2002) Identification of 30 protein species involved in replicative senescence and stress-induced premature senescence. FEBS Lett. 531, 499–504.

[4] Dumont, P., Burton, M., Chen, Q.M., Gonos, E.S., Frippiat, C., Mazarati, J.B., Eliaers, F., Remacle, J. and Toussaint, O. (2000) Induction of replicative senescence biomarkers by sublethal oxidative stresses in normal human fibroblast. Free Radic. Biol. Med. 28, 361–373.

[5] Dumont, P., Chainiaux, F., Eliaers, F., Petropoulou, C., Remacle, J., Koch-Brandt, C., Gonos, E.S. and Toussaint, O. (2002) Overexpression of apolipoprotein J in human fibroblasts protects against cytotoxicity and premature senescence induced by ethanol and *tert*-butylhydroperoxide. Cell Stress Chaperones 7, 23–35.

[6] Frippiat, C., Chen, Q.M., Zdanov, S., Magalhaes, J.P., Remacle, J. and Toussaint, O. (2001) Subcytotoxic H_2O_2 stress triggers a release of transforming growth factor-beta 1, which induces biomarkers of cellular senescence of human diploid fibroblasts. J. Biol. Chem. 276, 2531–2537.

[7] Rodemann, H.P., Bayreuther, K., Francz, P.I., Dittmann, K. and Albiez, M. (1989) Selective enrichment and biochemical characterization of seven human skin fibroblasts cell types in vitro. Exp. Cell Res. 180, 84–93.

[8] Debacq-Chainiaux, F., Borlon, C., Pascal, T., Royer, V., Eliaers, F., Ninane, N., Carrard, G., Friguet, B., de Longueville, F., Boffe, S., Remacle, J. and Toussaint, O. (2005) Repeated exposure of human skin fibroblasts to UVB at subcytotoxic level triggers premature senescence through the TGF-beta1 signaling pathway. J. Cell Sci. 118, 743–758.

[9] Brack, C., Lithgow, G., Osiewacz, H. and Toussaint, O. (2000) EMBO WORKSHOP REPORT: Molecular and cellular gerontology Serpiano, Switzerland, September 18–22, 1999. Embo J 19, 1929–1934..

[10] Doggett, D.L., Rotenberg, M.O., Pignolo, R.J., Phillips, P.D. and Cristofalo, V.J. (1992) Differential gene expression between young and senescent, quiescent WI-38 cells. Mech. Ageing Dev. 65, 239–255.

[11] Hara, E., Yamaguchi, T., Tahara, H., Tsuyama, N., Tsurui, H., Ide, T. and Oda, K. (1993) DNA-DNA subtractive cDNA cloning using oligo $(dT)_{30}$-Latex and PCR: identification of cellular genes which are overexpressed in senescent human diploid fibroblasts. Anal. Biochem. 214, 58–64.

[12] Hardy, K., Mansfield, L., Mackay, A., Benvenuti, S., Ismail, S., Arora, P., O'Hare, M.J. and Jat, P.S. (2005) Transcriptional networks and cellular senescence in human mammary fibroblasts. Mol. Biol. Cell 16, 943–953.

[13] Linskens, M.H., Feng, J., Andrews, W.H., Enlow, B.E., Saati, S.M., Tonkin, L.A., Funk, W.D. and Villeponteau, B. (1995) Cataloging altered gene expression in young and senescent cells using enhanced differential display. Nucleic Acids Res. 23, 3244–3251.

[14] Shelton, D.N., Chang, E., Whittier, P.S., Choi, D. and Funk, W.D. (1999) Microarray analysis of replicative senescence. Curr. Biol. 9, 939–945.

[15] Toussaint, O., Salmon, M., Royer, V., Dierick, J.-F., de Magalhaes, J.P., Wenders, F., Zdanov, S., Chrétien, A., Borlon, C., Pascal, T. and Chainiaux, F. (2003) Role of subcytotoxic stress in tissue ageing (Nyström, T. and Osiewacz, H.D., Eds.), Model Systems in Ageing, vol. 3, pp. 269–294, Springer-Verlag, Heidelberg.

[16] Liang, P. (2002) A decade of differential display. Biotechniques 33, 338–346.

[17] Liang, P. and Pardee, A.B. (1992) Differential display of eukaryotic messenger RNA by means of the polymerase chain reaction. Science 257, 967–971.

[18] de Longueville, F., Surry, D., Meneses-Lorente, G., Bertholet, V., Talbot, V., Evrard, S., Chandelier, N., Pike, A., Worboys, P., Rasson, J.P., Le Bourdelles, B. and Remacle, J. (2002) Gene expression profiling of drug metabolism and toxicology markers using a low-density DNA microarray. Biochem. Pharmacol. 64, 137–149.

[19] de Magalhaes, J.P., Chainiaux, F., de Longueville, F., Mainfroid, V., Migeot, V., Marcq, L., Remacle, J., Salmon, M. and Toussaint, O. (2004) Gene expression and regulation in H_2O_2-induced premature senescence of human foreskin fibroblasts expressing or not telomerase. Exp. Gerontol. 39, 1379–1389.

[20] Hayflick, L. and Moorhead, P.S. (1961) The serial cultivation of human diploid cell strains. Exp. Cell Res. 25, 585–621.

[21] Jesnowski, R., Backhaus, C., Ringel, J. and Lohr, M. (2002) Ribosomal highly basic 23-kDa protein as a reliable standard for gene expression analysis. Pancreatology 2, 421–424.

[22] Kayes-Wandover, K.M. and White, P.C. (2000) Steroidogenic enzyme gene expression in the human heart. J. Clin. Endocrinol. Metab. 85, 2519–2525.

[23] Marone, M., Mozzetti, S., De Ritis, D., Pierelli, L. and Scambia, G. (2001) Semiquantitative RT-PCR analysis to assess the expression levels of multiple transcripts from the same sample. Biol. Proced. Online 3, 19–25.

[24] Sturzenbaum, S.R. and Kille, P. (2001) Control genes in quantitative molecular biological techniques: the variability of invariance. Comp. Biochem. Physiol. B Biochem. Mol. Biol. 130, 281–289.

[25] Zammatteo, N., Jeanmart, L., Hamels, S., Courtois, S., Louette, P., Hevesi, L. and Remacle, J. (2000) Comparison between different strategies of covalent attachment of DNA to glass

surfaces to build DNA microarrays. Anal. Biochem. 280, 143–150.
[26] Humphreys, D.T., Carver, J.A., Easterbrook-Smith, S.B. and Wilson, M.R. (1999) Clusterin has chaperone-like activity similar to that of small heat shock proteins. J. Biol. Chem. 274, 6875–6881.
[27] Poon, S., Treweek, T.M., Wilson, M.R., Easterbrook-Smith, S.B. and Carver, J.A. (2002) Clusterin is an extracellular chaperone that specifically interacts with slowly aggregating proteins on their off-folding pathway. FEBS Lett. 513, 259–266.
[28] Kumazaki, T., Kobayashi, M. and Mitsui, Y. (1993) Enhanced expression of fibronectin during in vivo cellular aging of human vascular endothelial cells and skin fibroblasts. Exp. Cell Res. 205, 396–402.
[29] Funk, S.E. and Sage, E.H. (1991) The $Ca^{2(+)}$-binding glycoprotein SPARC modulates cell cycle progression in bovine aortic endothelial cells. Proc. Natl. Acad. Sci. USA 88, 2648–2652.
[30] Volonte, D., Zhang, K., Lisanti, M.P. and Galbiati, F. (2002) Expression of caveolin-1 induces premature cellular senescence in primary cultures of murine fibroblasts. Mol. Biol. Cell 13, 2502–2517.
[31] Cho, K.A. and Park, S.C. (2005) Caveolin-1 as a prime modulator of aging: a new modality for phenotypic restoration. Mech. Ageing Dev. 126, 105–110.
[32] Park, W.Y., Park, J.S., Cho, K.A., Kim, D.I., Ko, Y.G., Seo, J.S. and Park, S.C. (2000) Up-regulation of caveolin attenuates epidermal growth factor signaling in senescent cells. J. Biol. Chem. 275, 20847–20852.
[33] Frippiat, C., Dewelle, J., Remacle, J. and Toussaint, O. (2002) Signal transduction in H_2O_2-induced senescence-like phenotype in human diploid fibroblasts. Free Radic. Biol. Med. 33, 1334–1346.
[34] Martin, J.L. and Baxter, R.C. (1991) Transforming growth factor-beta stimulates production of insulin-like growth factor-binding protein-3 by human skin fibroblasts. Endocrinology 128, 1425–1433.
[35] Baxter, R.C. (2001) Signalling pathways involved in antiproliferative effects of IGFBP-3: a review. Mol. Pathol. 54, 145–148.
[36] Huang, S.S., Ling, T.Y., Tseng, W.F., Huang, Y.H., Tang, F.M., Leal, S.M. and Huang, J.S. (2003) Cellular growth inhibition by IGFBP-3 and TGF-beta1 requires LRP-1. Faseb J. 17, 2068–2081.
[37] Leal, S.M., Liu, Q., Huang, S.S. and Huang, J.S. (1997) The type V transforming growth factor beta receptor is the putative insulin-like growth factor-binding protein 3 receptor. J. Biol. Chem. 272, 20572–20576.
[38] Tseng, W.F., Huang, S.S. and Huang, J.S. (2004) LRP-1/TbetaR-V mediates TGF-beta1-induced growth inhibition in CHO cells. FEBS Lett. 562, 71–78.
[39] Crichton, R.R., Wilmet, S., Legssyer, R. and Ward, R.J. (2002) Molecular and cellular mechanisms of iron homeostasis and toxicity in mammalian cells. J. Inorg. Biochem. 91, 9–18.
[40] Lee, K.W., Liu, B., Ma, L., Li, H., Bang, P., Koeffler, H.P. and Cohen, P. (2004) Cellular internalization of insulin-like growth factor binding protein-3: distinct endocytic pathways facilitate re-uptake and nuclear localization. J. Biol. Chem. 279, 469–476.
[41] Noblesse, E., Cenizo, V., Bouez, C., Borel, A., Gleyzal, C., Peyrol, S., Jacob, M.P., Sommer, P. and Damour, O. (2004) Lysyl oxidase-like and lysyl oxidase are present in the dermis and epidermis of a skin equivalent and in human skin and are associated to elastic fibers. J. Invest Dermatol. 122, 621–630.
[42] Bringold, F. and Serrano, M. (2000) Tumor suppressors and oncogenes in cellular senescence. Exp. Gerontol. 35, 317–329.
[43] Collado, M., Medema, R.H., Garcia-Cao, I., Dubuisson, M.L., Barradas, M., Glassford, J., Rivas, C., Burgering, B.M., Serrano, M. and Lam, E.W. (2000) Inhibition of the phosphoinositide 3-kinase pathway induces a senescence-like arrest mediated by p27Kip1. J. Biol. Chem. 275, 21960–21968.
[44] Ryan, D.G., Taliana, L., Sun, L., Wei, Z.G., Masur, S.K. and Lavker, R.M. (2003) Involvement of S100A4 in stromal fibroblasts of the regenerating cornea. Invest. Ophthalmol. Vis. Sci. 44, 4255–4262.
[45] Bittles, A.H. and Harper, N. (1984) Increased glycolysis in ageing cultured human diploid fibroblasts. Biosci. Rep. 4, 751–756.
[46] Stein, G.H., Beeson, M. and Gordon, L. (1990) Failure to phosphorylate the retinoblastoma gene product in senescent human fibroblasts. Science 249, 666–669.